

# 基于 End-On 叠氮桥联的混合价 Co(II/III)和一维 Cu(II)链-席夫碱化合物的合成、结构及磁学性质

田菊梅<sup>\*1</sup> 张景萍<sup>2</sup>

<sup>1</sup> 厦门医学院口腔医学系, 厦门 361023

<sup>2</sup> 东北师范大学化学学院, 长春 130024

**摘要:** 合成了 2 个化合物  $[\text{Co}^{\text{II}}\text{Co}^{\text{III}}_4(\text{salhn})_4(\text{N}_3)_6(\text{CH}_3\text{OH})_2(\text{H}_2\text{O})_2] \cdot 4\text{CH}_3\text{OH} \cdot 2\text{H}_2\text{O}$  (**1**) 和  $[\text{Cu}_2(\text{salhn})(\text{N}_3)_2]_n$  (**2**) ( $\text{H}_2\text{salhn} = N, N'$ -bis(salicylidene)hydrazine), 并用 X 射线单晶衍射进行结构表征。化合物 **1** 是一个五核的  $[\text{Co}^{\text{II}}\text{Co}^{\text{III}}_4]$  钴簇, 而化合物 **2** 是一个具有结构单元为  $[\text{Cu}_2(\text{salhn})(\text{N}_3)_2]$  的一维链结构。2 个化合物中叠氮均具有 end-on( $\text{EO}, \mu-1, 1$ ) 的配位模式。化合物 **1** 和 **2** 的磁学性质测试表明它们都具有反铁磁行为。

**关键词:** 席夫碱; 叠氮; 反铁磁性; 晶体结构; 桥联配体

中图分类号: O614.81<sup>+</sup>2; O614.121

文献标识码: A

文章编号: 1001-4861(2018)03-0436-09

DOI: 10.11862/CJIC.2018.053

## Penta-nuclear Mixed-Valence Co(II/III) and 1D Chain Cu(II) Complexes Incorporating Schiff Base Ligand with End-On Azido Bridging: Syntheses, Structures and Magnetic Properties

TIAN Ju-Mei<sup>\*1</sup> ZHANG Jing-Ping<sup>2</sup>

<sup>1</sup>Department of Stomatology, Xiamen Medical College, Xiamen, Fujian 361023, China

<sup>2</sup>Faculty of Chemistry, Northeast Normal University, Changchun 130024, China

**Abstract:** Two novel complexes,  $[\text{Co}^{\text{II}}\text{Co}^{\text{III}}_4(\text{salhn})_4(\text{N}_3)_6(\text{CH}_3\text{OH})_2(\text{H}_2\text{O})_2] \cdot 4\text{CH}_3\text{OH} \cdot 2\text{H}_2\text{O}$  (**1**) and  $[\text{Cu}_2(\text{salhn})(\text{N}_3)_2]_n$  (**2**) ( $\text{H}_2\text{salhn} = N, N'$ -bis(salicylidene)hydrazine), were synthesized and structurally characterized by X-ray single-crystal diffraction. Complex **1** is a zigzag-like penta-nuclear  $[\text{Co}^{\text{II}}\text{Co}^{\text{III}}_4]$  cobalt cluster, while complex **2** consists of a 1D chain containing subunit  $[\text{Cu}_2(\text{salhn})(\text{N}_3)_2]$ . Both complexes possess bridged azide with the end-on ( $\text{EO}, \mu-1, 1$ ) coordination fashion. The magnetic measurements indicate that **1** and **2** both show antiferromagnetic behaviors. CCDC: 869426, **1**; 869427, **2**.

**Keywords:** Schiff base; azido group; antiferromagnetism; crystal structure; bridging ligand

The design of molecule-based magnetic materials is one of the hot topics owing to their potential applications including high-density information storage, quantum information computing technology, spintronic and magnetocaloric refrigeration<sup>[1-13]</sup>. Magnetic materials can display attractive architecture and magnetic

exchange coupling due to their tunable characteristics by employing well established design principle and synthetic procedure<sup>[14-17]</sup>. There are many factors influencing the target magnetic complexes during the course of synthesis, such as well-designed polydentate ligands, bridging ligands, transition metal ions, solvent, temp-

收稿日期: 2017-08-21。收修改稿日期: 2017-10-30。

福建省卫生计生青年科研课题(No.2017-2-115)、厦门医学院内科研平台课题(No.KYPT2015-02)和厦门医学高等专科学校自然科学基金项目(No.K2015-13)资助。

\*通信联系人。E-mail: tjm@xmmc.edu.cn

erature, stoichiometric ratio, pH value, crystallization mechanism and the order of addition. Our present work has focused on investigating the influence of bridging ligands on the molecular structure dimension and magnetic properties of the resulting system, and exploring the magneto-structural correlations.

According to the reported literature, we find that the ligand diazine Schiff base  $N,N'$ -bis(salicylidene)hydrazine ( $H_2salhn$ ) is especially useful in forming mono-/dinuclear metal complexes, *e.g.*, dinuclear  $3d$  metal complexes  $M_2(salhn)_3$  ( $M=Fe, Co, Mn$ )<sup>[18-21]</sup>, dinuclear zinc and copper complex  $M_2(salhn)_2(H_2O)_4$  ( $M=Zn, Cu$ )<sup>[22]</sup>, mononuclear ruthenium complex  $[RuH(CO)(PPh_3)_2(salhn)]$ <sup>[23]</sup>, series of di-ruthenium complexes<sup>[24]</sup>, dirhodium  $[(CO)_2Rh(salhn)Rh(CO)_2]$ <sup>[25]</sup>. The  $N_2O_2$ -donor Schiff base  $H_2salhn$  provides the =N-N= fragment, which acts not only as chelating sites, but also as bridging unit between the two metal ions<sup>[20]</sup>. Therefore,  $H_2salhn$  is inclined to act as a role of chelating ligands, and thus to form two nuclear clusters. This allows us to consider employing other bridging ligands, which may be helpful to assemble extended system (from 0D to 1D or 2D or 3D) and to investigate the related magnetic properties of the resulting novel systems.

Therefore, a suitable bridging ligand plays a crucial role in assembling extended magnetic materials of the Schiff base  $H_2salhn$  system. In our previous work<sup>[26-27]</sup>, our group has assembled magnetic materials by selecting carboxylate bridging ligands to bind  $3d$  transition-metal ions into polynuclear aggregates. As the expansion of this line, the azido ligand is another suitable choice as bridging ligand for the construction of magnetic materials due to their extremely versatile coordination modes and effectively mediating magnetic exchange interactions<sup>[28-38]</sup>. Herein, we have successfully synthesized and studied two novel complexes  $[Co^{II}Co^{III}_4(salhn)_4(N_3)_6(CH_3OH)_2(H_2O)_2] \cdot 4CH_3OH \cdot 2H_2O$  (**1**) and  $[Cu_2(salhn)(N_3)_2]_n$  (**2**). Complex **1** consists of a mixed-valence penta-nuclear cobalt cluster. Compared with the previous  $Co_2(salhn)_3$  diamagnetic system<sup>[20]</sup>, complex **1** shows antiferromagnetic behaviors according to the magnetic measurements. Complex **2** consists of a 1D copper chain, in which the azido groups successfully replace coor-

minated water molecules to form extended network by using different synthetic method as compared to the reported  $Cu_2(salhn)_2(H_2O)_4$  system<sup>[22]</sup>. In these two complexes, azido groups both adopt end-on (EO,  $\mu$ -1, 1) coordination mode. The magnetic measurements indicate complex **2** shows antiferromagnetic behavior. Here, we have reported the synthesis, X-ray single-crystal structure, and magnetic properties of these two complexes.

## 1 Experimental

### 1.1 Reagents and physical measurements

**Caution!** The reported azide is potentially explosive. Only small amounts of the material should be handled, and with care.

Solvents and starting materials were purchased commercially and used as received without further purification unless otherwise noted. The Schiff base  $H_2salhn$  was prepared in ~95% yield by condensation reaction of hydrazine and salicylaldehyde in a 1:2 molar ratio in methanol according to the reported method<sup>[19]</sup>. The resulted yellow precipitate followed by recrystallization from dimethylformamide (DMF) to form yellow single crystal of  $H_2salhn$  suited for X-ray diffraction analysis, which crystallizes in the monoclinic space group  $P2_1/n$  with the crystallographic parameter:  $a=8.526\ 0(19)$  nm,  $b=6.319\ 0(14)$  nm,  $c=11.823(3)$  nm,  $\beta=107.846(3)^\circ$ .

The elemental analyses (C, H, and N) were performed on a Perkin-Elmer Model 240C elemental analyzer. The Cu and Co elemental analyses were determined by the Leaman inductively coupled plasma (ICP) spectrometer. Infrared spectra ( $400\sim 4\ 000\ cm^{-1}$ ) were measured on a Perkin-Elmer Fourier transform infrared (FTIR) spectrophotometer using KBr pellets. Powder X-ray diffraction (PXRD) measurements were assessed on a Siemens D5005 diffractometer with  $Cu\ K\alpha$  ( $\lambda=0.154\ 184\ nm$ ) with a step size of  $0.1^\circ$  in  $2\theta$  range of  $5^\circ\sim 50^\circ$  at room temperature. The XRD accelerating voltage and emission current were 40 kV and 30 mA, respectively.

### 1.2 Syntheses of complexes 1~2

1.2.1 Synthesis of  $[Co^{II}Co^{III}_4(salhn)_4(N_3)_6(CH_3OH)_2(H_2O)_2] \cdot 4CH_3OH \cdot 2H_2O$  (**1**)

$H_2salhn$  (0.24 g, 1 mmol) and KOH (0.11 g, 2

mmol) were dissolved in methanol solvent (20 mL), forming a clear yellow solution, which was magnetically stirred at 40~50 °C for 30 min. Then, a methanol solution (20 mL) of  $\text{CoCl}_2 \cdot 6\text{H}_2\text{O}$  (0.71 g, 3 mmol) was added to the hot yellow solution. After 15 min, an aqueous solution (1 mL) of sodium azide (0.20 g, 3 mmol) was added under continuous stirring for 1 h. Black-colored, needle-like crystals of complex **1** were obtained from the filtrate after a few days. Yield: 65% (based on Co ions). Anal. Calcd. for  $\text{C}_{62}\text{H}_{72}\text{Co}_5\text{N}_{26}\text{O}_{18}$  (%): Co, 16.70; C, 42.21; H, 4.11; N, 20.64. Found (%): Co, 17.10; C, 41.82; H, 4.28; N, 20.14. IR (KBr,  $\text{cm}^{-1}$ ): 2 077 and 2 023 for the azido groups, 1 603 for  $\nu(\text{C}=\text{N})$ .

### 1.2.2 Synthesis of $[\text{Cu}_2(\text{salhn})(\text{N}_3)_2]_n$ (**2**)

An aqueous solution (1 mL) of sodium azide (0.039 g, 0.6 mmol) was added to a methanol solution (20 mL) of  $\text{Cu}(\text{NO}_3)_2 \cdot 3\text{H}_2\text{O}$  (0.097 0.4 mmol). After stirring for 20 min, a hot DMF solution (2 mL) of  $\text{H}_2\text{salhn}$  (0.048 g, 0.2 mmol) and triethylamine (0.040 g, 0.4 mmol) was added to the resulting mixture with continuous stirring for 3 h. Black-colored, block crystals of **2** were obtained from the filtrate after a few

days. Yield: 60% (based on Cu ions). Anal. Calcd. for  $\text{C}_{14}\text{H}_{10}\text{Cu}_2\text{N}_8\text{O}_2$  (%): Cu, 28.28; C, 37.42; H, 2.24; N, 24.94. Found(%): Cu, 28.34; C, 37.12; H, 2.29; N, 24.44. IR (KBr,  $\text{cm}^{-1}$ ): 2 046 and 2 101 for the azido groups, 1 604 for  $\nu(\text{C}=\text{N})$ .

### 1.3 Details of X-ray crystallography

Single-crystal X-ray diffraction data sets for **1** and **2** were obtained on a Bruker SMART APEX CCD area detector diffractometer using graphite monochromated Mo  $K\alpha$  radiation ( $\lambda=0.071\ 073\ \text{nm}$ ) at 195 K. Structure solution (direct methods) and the refinement of full-matrix least-squares were carried out using the SHELXTL software package<sup>[39]</sup>. All the non-hydrogen atoms were refined with anisotropic thermal parameters. The hydrogen atoms attached to carbon and nitrogen atoms were placed in geometrically calculated positions. Crystallographic and refinement details for all compounds are summarized in Table 1. Selected bond lengths and angles are listed in Table S1 ~S2 (Supporting information).

CCDC: 869426, **1**; 869427, **2**.

### 1.4 Magnetic measurements

The magnetic susceptibility measurements on

Table 1 Crystallographic data and structure refinement summary for complexes **1**~**2**

	<b>1</b>	<b>2</b>
Formula	$\text{C}_{62}\text{H}_{72}\text{Co}_5\text{N}_{26}\text{O}_{18}$	$\text{C}_{14}\text{H}_{10}\text{Cu}_2\text{N}_8\text{O}_2$
Formula weight	1 764.11	449.38
Space group	$P2_1/n$	$P2_1/n$
Crystal system	Monoclinic	Monoclinic
$a / \text{nm}$	1.244 40(9)	0.603 10(8)
$b / \text{nm}$	1.534 30(11)	1.541 8(2)
$c / \text{nm}$	1.981 60(14)	1.721 8(2)
$\beta / (^\circ)$	98.956 0(12)	97.151 0(18)
$V / \text{nm}^3$	3.737 3(5)	1.588 6(4)
$Z$	2	4
$D_c / (\text{g} \cdot \text{cm}^{-3})$	1.568	1.879
Absorption coefficient / $\text{mm}^{-1}$	1.172	2.707
$F(000)$	1 810	896
$\theta$ range / $(^\circ)$	1.686~25.044	1.779~25.08
Unique reflection ( $R_{\text{int}}$ )	6 616 (0.040 7)	2 833 (0.024 2)
$R_1^a, wR_2^b [I > 2\sigma(I)]$	0.042 1, 0.089 2	0.032 5, 0.079 1
$R_1^a, wR_2^b$ (all data)	0.058 6, 0.096 8	0.038 7, 0.082 1
GOF on $F^2$	1.025	1.043

<sup>a</sup> $R = \sum ||F_o| - |F_c|| / \sum |F_o|$ ; <sup>b</sup> $wR_2 = [\sum w(|F_o| - |F_c|)^2 / \sum w(F_o^2)]^{1/2}$ ;  $w = 1/(\sigma F_o^2)$ .

polycrystalline samples of **1** and **2** were conducted on Quantum Design SQUID MPMS XL-5 instruments in the temperature range of 300~2 K and under the applied magnetic field of 1 and 5 kOe, respectively. The field dependent magnetizations for **1** and **2** were measured at 2 K in the field range of 0~5 T. The temperature dependence of the field-cooled (FC), zero-field-cooled (ZFC) for **2** was assessed under a dc field of 100 Oe.

## 2 Results and discussion

### 2.1 Synthesis

Complex **1** has been synthesized by reacting  $\text{CoCl}_2 \cdot 6\text{H}_2\text{O}$ ,  $\text{H}_2\text{salhn}$ ,  $\text{KOH}$ , and  $\text{NaN}_3$  in 3:1:2:3 molar ratio in the mixture solvent (41 mL) of methanol and water (40:1, V/V). The trivalent cobalt may be resulted from the oxidation of Co(II) to Co(III) by atmospheric oxygen gas under basic condition. Excess of metal material may be responsible to the presence of divalent cobalt center in complex **1**, compared to

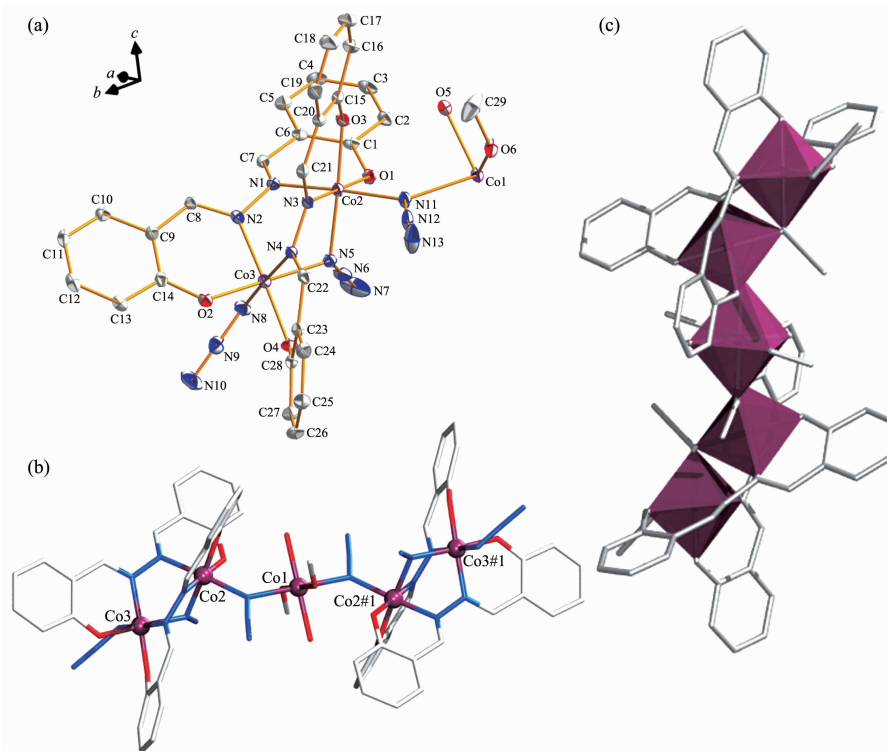
the full trivalent metal system  $\text{Co}_2(\text{salhn})_3$  assembling from  $\text{CoCl}_2 \cdot 6\text{H}_2\text{O}$ ,  $\text{H}_2\text{salhn}$ ,  $\text{KOH}$  in 2:3:6 molar ratio<sup>[20]</sup>.

A mixture solvent (methanol 20 mL, DMF 2 mL and water 1 mL) of  $\text{Cu}(\text{NO}_3)_2 \cdot 3\text{H}_2\text{O}$ ,  $\text{H}_2\text{salhn}$ ,  $\text{NaN}_3$ , and triethylamine in 2:1:3:2 molar ratio yields block crystals of **2**.

### 2.2 X-ray crystal structures

#### 2.2.1 Structural analyses of **1**

Single-crystal X-ray diffraction analysis indicates that complex **1** crystallizes in the monoclinic space group  $P2_1/n$ . The selected bond distances and bond angles are given in Table S1. The molecule is a neutral zigzag-like penta-nuclear cobalt cluster. And four  $\text{CH}_3\text{OH}$  molecules and two  $\text{H}_2\text{O}$  molecules are located in the crystal lattice. The asymmetric unit consists of three Co ions, two deprotonated ligands ( $\text{salhn}^{2-}$ ), two end-on azido groups, one terminal azido group, one coordinated  $\text{H}_2\text{O}$  molecule and  $\text{CH}_3\text{OH}$  molecule (Fig.1a). Co(1) is located on an inversion centre and exhibits a  $\text{N}_2\text{O}_4$  coordination polyhedron



Hydrogen atoms are omitted for clarity; Solvent molecules in the crystal lattice are not shown for clarity;  
Symmetry codes: #1:  $-x, -y+1, -z$

Fig.1 Structure of complex **1**: (a) ellipsoid of the subunit and the numbering scheme with probability of 30%; (b) penta-nuclear cobalt cluster and the numbering scheme for cobalt ions viewing from the same direction as (a); (c) zigzag-like cluster along  $a$  axis

with octahedral geometry. Two nitrogen atoms from two azido groups are situated at axial positions. The equatorial positions are occupied by four oxygen atoms belonging to two coordinated  $\text{H}_2\text{O}$  molecules and  $\text{CH}_3\text{OH}$  molecules, respectively. The azido group acts as the only bridge between  $\text{Co}(1)$  and  $\text{Co}(2)$  with the bond angle  $\text{Co}(1)\text{-N}(11)\text{-Co}(2)$ ,  $131.89^\circ$  and the  $\text{Co}(1)\cdots\text{Co}(2)$  distance,  $0.374\ 7\ \text{nm}$ . The two phenolate oxygens of  $\text{H}_2\text{salhn}$  are deprotonated acting as a quadridentate ( $\text{N}_2\text{O}_2$ ) dianion containing two nitrogen atoms from diazine ( $=\text{N-N}=\text{}$ ) binding two metal ions  $\text{Co}(2)$  and  $\text{Co}(3)$ . The other two sites for  $\text{Co}(2)$  and  $\text{Co}(3)$  have been taken up by nitrogen atoms from azido anions. It is worth noting that a reference of charge balance as well as an analysis of the  $\text{Co-N}$  and  $\text{Co-O}$  bond lengths, which are longer for  $\text{Co}(1)$  (with  $0.213\ 5$  and  $0.207\ 2\sim 0.207\ 9\ \text{nm}$ , respectively) than for  $\text{Co}(2)$  and  $\text{Co}(3)$  (with  $0.191\ 4\sim 0.196\ 7\ \text{nm}$  and  $0.187\ 9\sim 0.189\ 8\ \text{nm}$ , respectively), clearly indicate the presence of mixed valence cobalt ions. The  $+2$  valence state is assigned to  $\text{Co}(1)$ , while the  $+3$  valence state is

assigned to  $\text{Co}(2)/\text{Co}(3)$  and their symmetry related  $\text{Co}(2)\#1/\text{Co}(3)\#1$ , which are also confirmed by bond valence sum (BVS) calculations<sup>[20,40-41]</sup>.

### 2.2.2 Structural analyses of **2**

Complex **2** crystallizes in the monoclinic space group  $P2_1/n$ , and the asymmetric unit consists of two crystallographically independent Cu atoms, one  $\text{salhn}^{2-}$  ligand, and two  $\text{N}_3^-$  groups (Fig.2a). Ligand  $\text{H}_2\text{salhn}$  acts as a quadridentate ( $\text{N}_2\text{O}_2$ ) biantion ( $\text{salhn}^{2-}$ ) linked through two imine N atoms and two deprotonated phenoxide O atoms. In the dimer unit, each Cu ion is penta-coordinate to form a distorted square pyramidal coordination environment. The Addison parameter ( $\tau$ ) is  $0.06$  for  $\text{Cu}(1)$  and  $0.22$  for  $\text{Cu}(2)$  ( $\tau$  is equal to zero for a perfect square-pyramidal geometry, while it is one for an ideal trigonal bipyramidal geometry)<sup>[42]</sup>. Each Cu ion is coordinated by two N atoms from two different azido groups, one N atom from one  $\text{salhn}^{2-}$  ligand, and two oxygen atoms from two different  $\text{salhn}^{2-}$  ligands. Within the dimer, a triplicate bridge between  $\text{Cu}(1)$  and  $\text{Cu}(2)$  is made by two phenoxide O

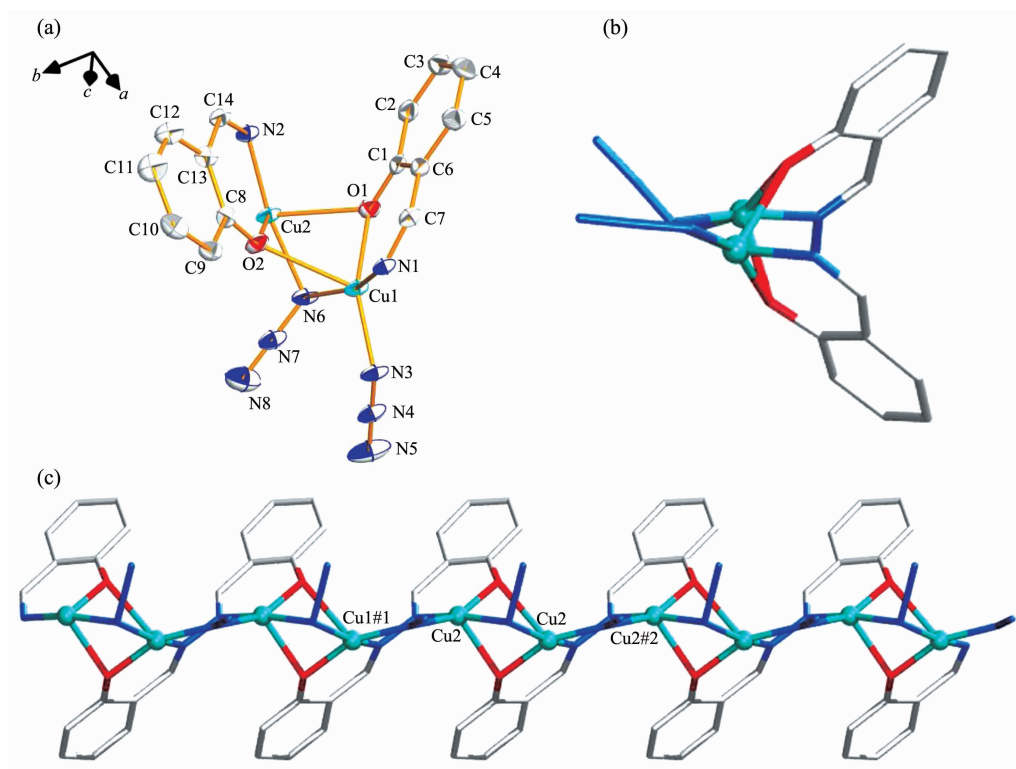


Fig.2 Structure of complex **2**: ellipsoid of the dimer and the numbering scheme with probability of 50%(a); 1D chain along  $a$  axis (b), or  $c$  axis (c)



atoms(O(1), O(2)) from two  $\text{salhn}^{2-}$  ligands and one EO ( $\mu$ -1, 1) azido N atom N(6). The two phenoxide-O (O(1), O(2)) show different bridge angles ( $\angle \text{Cu}(1)\text{-O}(1)\text{-Cu}(2) = 83.48^\circ$  and  $\angle \text{Cu}(1)\text{-O}(2)\text{-Cu}(2) = 79.11^\circ$ ). The bridge angle through azido N atom (Cu(1)-N(6)-Cu(2)) is  $89.77^\circ$ . The Cu(1)···Cu(2) distance within the dimer is 0.285 4(6) nm, but the inter-dimer Cu···Cu distance is 0.336 9 nm. The Cu-O and Cu-N bond distances lie in the range of 0.192 0(2)~0.234 1(2) nm and 0.194 8(3)~0.202 9(3) nm, respectively. The selected bond distances and bond angles are given in Table S2.

Inspection of the structure of the 1D chain shows a scissor-shaped structure running along  $a$  axis (Fig.2b and 2c). The adjacent chains are packing along  $a$  axis through C(3)-H(3)···O(2) and C(14)-H(14)···N(5) hydrogen bonding interactions (Fig.3). The hydrogen bond C(3)-H(3)···O(2) involves C-H fragment of a benzene ring and the O-atom of phenolate with C(3)···O(2) distance of 0.343 1 nm and C(3)-H(3)···O(2) angle of  $135.61^\circ$ . The another hydrogen bond C(14)-H(14)···N(5) involves C-H fragment of methylene group and the N-atom of azido group with C(14)···N(5) distance of 0.345 9 nm and C(14)-H(14)···N(5) angle

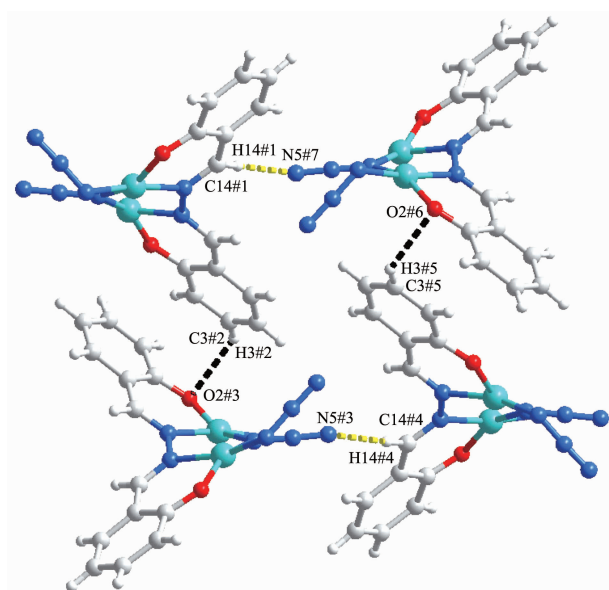
of  $177.0^\circ$ .

## 2.2 IR spectroscopy and PXRD properties

As depicted in Fig.S1, a strong stretching band at  $1\,625\text{ cm}^{-1}$  indicates the presence of imine group C=N stretching for ligand  $\text{H}_2\text{salhn}$ , which is in agreement with the crystal structure. However, the imine stretching appears at  $1\,603\text{ cm}^{-1}$  for **1** and  $1\,604\text{ cm}^{-1}$  for **2**, which may be resulted from the effect of N atom coordination with metal. The similar trend can be found in the reported other metal coordination complexes possessing the same ligand<sup>[19-20]</sup>. The characteristic azido stretching bands are found at  $2\,023$  and  $2\,077\text{ cm}^{-1}$  for **1** as well as  $2\,101$  and  $2\,046\text{ cm}^{-1}$  for **2**, which are typical for EO( $\mu$ -1, 1) azido bridging<sup>[32,43]</sup>. The purity of bulky samples of **1** (Fig.S2) and **2** (Fig.S3) were corroborated by the similarities between simulated and experimental PXRD patterns.

## 2.4 Magnet behaviour

Variable temperature dc susceptibility measurements of **1** and **2** were collected in the temperature range of 300~2 K under an applied field of 1 000 and 5 000 Oe, respectively. From a magnetic point of view, complex **1** is effectively mononuclear Co(II) system because the Co(III) sites are diamagnetic. As shown in Fig.4a, the  $\chi_m T$  value at room temperature for **1** is  $2.97\text{ cm}^3 \cdot \text{mol}^{-1} \cdot \text{K}$ , much higher than the spin-only high spin Co(II) ( $S=3/2$ ) value of  $1.875\text{ cm}^3 \cdot \text{mol}^{-1} \cdot \text{K}$  with  $g=2.0$ . This is probably induced by the presence of orbital contribution in octahedral Co(II) ion<sup>[44-45]</sup>. Upon cooling, the  $\chi_m T$  value first slightly decreases to a minimum value of  $2.15\text{ cm}^3 \cdot \text{mol}^{-1} \cdot \text{K}$  at 22 K. Below 22 K,  $\chi_m T$  value increases slightly to reach a maximum of  $2.19\text{ cm}^3 \cdot \text{mol}^{-1} \cdot \text{K}$  at 14 K, and secondly drops abruptly to a minimum value of  $1.57\text{ cm}^3 \cdot \text{mol}^{-1} \cdot \text{K}$  at 2 K. Fitting the data above 100 K with the Curie-Weiss law gives the Curie constant  $C=3.23\text{ cm}^3 \cdot \text{mol}^{-1} \cdot \text{K}$  and Weiss temperature  $\theta=-22.35\text{ K}$  (line in Fig.4a). The large negative Weiss constant value and the first decrease of  $\chi_m T$  above 22 K both indicate the occurrence of significant spin-orbital coupling and zero field splitting (ZFS) of the anisotropic HS Co(II) ion<sup>[46-48]</sup>. The sharp increase between 22 and 14 K could be due to the presence of impurity and the



Symmetry codes: #1:  $1+x, y, 1+z$ ; #2:  $x, y, 1+z$ ; #3:  $0.5-x, -0.5+y, 1.5-z$ ; #4:  $-x, -y, 1-z$ ; #5:  $1-x, -y, 1-z$ ; #6:  $0.5+x, 0.5-y, 0.5+z$ ; #7:  $-0.5+x, 0.5-y, 0.5+z$

Fig.3 Packing view of **2** formed by interchain hydrogen bond C(3)-H(3)···O(2) and C(14)-H(14)···N(5) along  $a$  axis

second decrease of  $\chi_m T$  below 14 K suggests the intermolecular antiferromagnetic interaction. The magnetization versus field plot at 2 K also confirms the observed antiferromagnetism (Fig.4b). At 5 T, the magnetization amounts to  $1.68N\beta$ , which is not saturated and is away from the theoretical value of  $3N\beta$  assuming  $g=2$ .

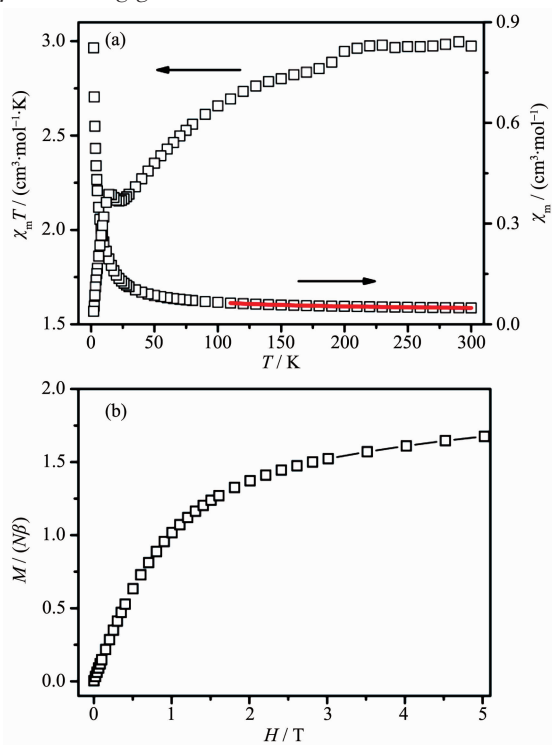


Fig.4 (a)  $\chi_m T$  vs  $T$  and  $\chi_m$  vs  $T$  plots in the temperature range of 2~300 K under a 1 000 Oe applied field; (b) Magnetization vs field plot at 2.0 K among 0~7 T for **1**

The  $\chi_m T$  value of complex **2** at room temperature is  $0.99 \text{ cm}^3 \cdot \text{mol}^{-1} \cdot \text{K}$ , which is larger than the spin-only value of  $0.75 \text{ cm}^3 \cdot \text{mol}^{-1} \cdot \text{K}$  calculated for two Cu(II) ions with  $g=2$  (Fig.5a). As the temperature is decreased, the  $\chi_m T$  value shows a slight decrease to a value of  $0.93 \text{ cm}^3 \cdot \text{mol}^{-1} \cdot \text{K}$  at 100 K, before an abrupt decrease to reach a value of *ca.*  $0.046 \text{ cm}^3 \cdot \text{mol}^{-1} \cdot \text{K}$  at 2.0 K. A fitting of the data above 100 K to Curie-Weiss law gives  $C=1.03 \text{ cm}^3 \cdot \text{mol}^{-1} \cdot \text{K}$  and  $\theta=-11.34 \text{ K}$  (line in the lower part of Fig.5a). The negative Weiss temperature and the decrease of  $\chi_m T$  both indicate a predominant antiferromagnetic interaction. Inspection of the structure suggests two different Cu...Cu interactions combining with two different Cu...N<sub>EO</sub>...

Cu angles (detailed describing in the structure part). We try to use two models: (i) alternating  $S=1/2$  antiferromagnetic chain; (ii) regular  $S=1/2$  antiferromagnetic chain model<sup>[42,49]</sup>. Unfortunately, these two models are not able to reproduce the magnetic properties adequately. Finally we have fitted the magnetic properties to the Ising model for 1D chain<sup>[49]</sup> (line in the upper part top of Fig.5a). This model reproduces the magnetic property of **2** extremely well with  $g=2.32$  and  $J=-23.49 \text{ cm}^{-1}$ . The field dependence of the magnetization for **2** is displayed in Fig.5b. The magnetization data does not reach the saturation value of  $2.0N\beta$  at 5 T, but equals  $0.15N\beta$ , which further confirms the strong antiferromagnetic interaction. Divergence of the ZFC and FC susceptibilities was observed below 50 K indicating a possible long-range ordered (Fig.6).

For copper(II) azido complexes, the different azido bridged fashion may mediate the different magnetic interaction. There are two cases for end-on azido bridged<sup>[29,34,36,50]</sup>: (i) the Cu-N<sub>EO</sub>-Cu angle is lower than

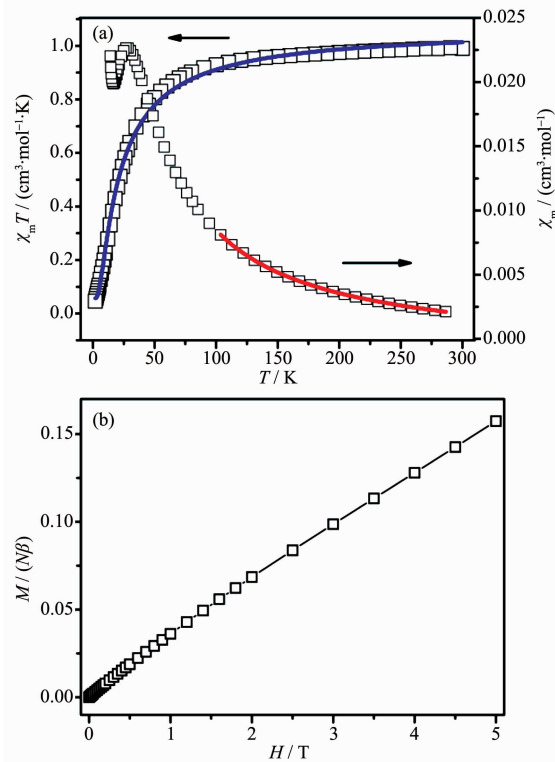


Fig.5 (a)  $\chi_m T$  vs  $T$  and  $\chi_m$  vs  $T$  plots in the temperature range of 2~300 K under a 5 000 Oe applied field; (b) Magnetization vs field plot at 2.0 K among 0~7 T for **2**

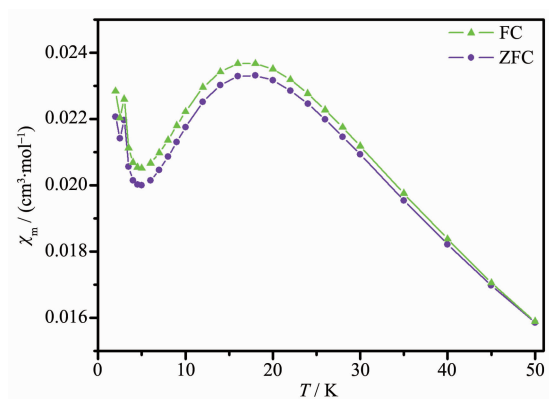


Fig.6 ZFC and FC as function of temperature at  $H=100$  Oe for **2**

$104^\circ$  (theory) or  $108^\circ$  (experiment), which propagates ferromagnetic; otherwise, it is antiferromagnetic. (ii) The longer bond distance of Cu-N<sub>3</sub> (EO) may lead to the weaker ferromagnetic interaction. In complex **2**, there are two different transition angle ( $\angle \text{Cu}(1)\text{-N}(6)\text{-Cu}(2)=89.77^\circ$  and  $\angle \text{Cu}(1)\text{-N}(3)\text{-Cu}(2)\#1=117.02^\circ$ ), which may propagate ferromagnetic and antiferromagnetic coupling, respectively. But the long bond distance (Cu(1)-N(6) 0.201 5 nm and Cu(2)-N(6) 0.202 9 nm) may weaken the ferromagnetic coupling. Therefore, the whole 1D chain behaves antiferromagnetic interaction.

### 3 Conclusions

In conclusion, we used azide as bridging group and successfully assembled two EO azido bridged complexes **1** and **2**, which both show antiferromagnetic behaviors. Compared with the reported metal-H<sub>2</sub>salhn complexes<sup>[20,22]</sup>, the azido groups within the complex successfully bridge the metal ions to form the extended structure and mediate the magnetic interaction. Further investigating other bridging ligand, such as cyano, oxalate, nitride, etc, which mediate magnetic interaction of other metal Schiff base complexes, is in progress in our group.

Supporting information is available at <http://www.wjhxxb.cn>

### References:

[1] Mazzanti M. *Nat. Chem.*, **2011**,**3**:426-427

- [2] Li B, Zhang J P, Zhang Y, et al. *CrystEngComm*, **2011**,**13**: 418-420
- [3] Mougél V, Chatelain L, Pécaut J, et al. *Nat. Chem.*, **2012**,**4**: 1011-1017
- [4] Mills D P, Moro F, McMaster J, et al. *Nat. Chem.*, **2011**,**3**: 454-460
- [5] Das A, Gieb K, Krupskaya Y, et al. *J. Am. Chem. Soc.*, **2011**,**133**:3433-3443
- [6] Sanvito S. *Chem. Soc. Rev.*, **2011**,**40**:3336-3355
- [7] Peng J B, Zhang Q C, Kong X J, et al. *Angew. Chem. Int. Ed.*, **2011**,**50**:10649-10652
- [8] Peng J B, Zhang Q C, Kong X J, et al. *J. Am. Chem. Soc.*, **2012**,**134**:3314-3317
- [9] Coronado E, Giménez-Marqués M, Espallargas G M, et al. *Nat. Commun.*, **2012**,**3**:828-835
- [10] Yoshida H, Yamaura J, Isobe M, et al. *Nat. Commun.*, **2012**,**3**: 860-864
- [11] Choubey S, Bhar K, Chattopadhyay S, et al. *Dalton Trans.*, **2012**,**41**:11551-11554
- [12] CHEN Yan-Min(陈延民), JIANG Yan(姜岩), HONG Si-Yu(洪思雨), et al. *Chinese J. Inorg. Chem.*(无机化学学报), **2017**,**33**(6):1023-1029
- [13] Seki H, Hosaka Y, Saito T, et al. *Angew. Chem. Int. Ed.*, **2016**,**55**:1360-1363
- [14] Talham D R, Meisel M W. *Chem. Soc. Rev.*, **2011**,**40**:3356-3365
- [15] HU Peng(胡鹏), XIAO Feng-Ping(肖凤屏), ZHI Zhong-Qiang(植中强), et al. *Chinese J. Inorg. Chem.*(无机化学学报), **2017**,**33**(7):1273-1279
- [16] Li Z Y, Ohtsu H, Kojima T, et al. *Angew. Chem. Int. Ed.*, **2016**,**55**:5184-5189
- [17] Friedländer S, Liu J, Addicoat M, et al. *Angew. Chem. Int. Ed.*, **2016**,**55**:12683-12687
- [18] Jian F F, Zhu C Y, Xiao H L, et al. *Z. Anorg. Allg. Chem.*, **2005**,**631**:769-772
- [19] Saroja J, Manivannan V, Chakraborty P, et al. *Inorg. Chem.*, **1995**,**34**:3099-3101
- [20] Sreerama S G, Pal S. *Inorg. Chem.*, **2005**,**44**:6299-6307
- [21] Mo H, Fang C J, Duan C Y, et al. *Dalton Trans.*, **2003**: 1229-1234
- [22] Aggarwal R C, Singh N K, Singh R P. *J. Indian Chem. Soc.*, **1986**,**63**:466
- [23] Trivedi M, Chandra M, Pandey D S, et al. *J. Organomet. Chem.*, **2004**,**689**:879-882
- [24] Singh S K, Chandra M, Pandey D S. *J. Organomet. Chem.*, **2004**,**689**:2073-2079
- [25] Gopinathan S, Pardhy S A, Gopinathan C, et al. *Inorg. Chim. Acta*, **1986**,**111**:133-138



- [26]Cui S X, Zhao Y L, Zhang J P, et al. *Polyhedron*, **2009**,**28**: 980-986
- [27]Cui S X, Zhao Y L, Zhang J P, et al. *Synth. Met.*, **2009**,**159**: 2191-2193
- [28]Hao Z M, Zhang X M. *Dalton Trans.*, **2011**,**40**:2092-2098
- [29]Zeng Y F, Hu X, Liu F C, et al. *Chem. Soc. Rev.*, **2009**,**38**: 469-480
- [30]Kang L C, Chen X, Wang X S, et al. *Dalton Trans.*, **2011**, **40**:5200-5209
- [31]Naiya S, Biswas C, Drew M G B, et al. *Inorg. Chem.*, **2010**, **49**:6616-6627
- [32]Tandon S S, Bunge S D, Motry D, et al. *Inorg. Chem.*, **2009**, **48**:4873-4881
- [33]Mukherjee S, Gole B, Chakrabarty R, et al. *Inorg. Chem.*, **2009**,**48**:11325-11334
- [34]Tian C B, Li Z H, Lin J D, et al. *Eur. J. Inorg. Chem.*, **2010**: 427-437
- [35]Zhang L F, Yu M M, Ni Z H, et al. *J. Mol. Struct.*, **2011**, **1006**:629-634
- [36]Gao Q, Xie Y B, Thorstad M, et al. *CrystEngComm*, **2011**, **13**:6787-6793
- [37]Weng D F, Wang Z M, Gao S. *Chem. Soc. Rev.*, **2011**,**40**: 3157-3181
- [38]Wang S, Zuo J L, Gao S, et al. *J. Am. Chem. Soc.*, **2004**, **126**:8900-8901
- [39]Sheldrick G M. *SHELXS-97* and *SHELXL-97*, University of Göttingen, Germany, **1997**.
- [40]Tandon S S, Bunge S D, Rakosi R, et al. *Dalton Trans.*, **2009**:6536-6551
- [41]Alley K G, Bircher R, Waldmann O, et al. *Inorg. Chem.*, **2006**,**45**:8950-8957
- [42]Adhikary C, Koner S. *Coord. Chem. Rev.*, **2010**,**254**:2933-2958
- [43]Demeshko S, Leibel G, Maringgele W, et al. *Inorg. Chem.*, **2005**,**44**:519-528
- [44]Nagaraja C M, Kumar N, Maji T K, et al. *Eur. J. Inorg. Chem.*, **2011**:2057-2063
- [45]Karasawa S, Koga N. *Inorg. Chem.*, **2011**,**50**:2055-2057
- [46]Li B, Zhang J P, Yong X, et al. *Dalton Trans.*, **2011**,**40**:4459-4464
- [47]Vallejo J, Castro I, Ruiz-García R, et al. *J. Am. Chem. Soc.*, **2012**,**134**:15704-15707
- [48]Han Y, Xu H, Liu Y, et al. *Chem. Eur. J.*, **2012**,**18**:13954-13958
- [49]Kahn O. *Molecular Magnetism*. New York: Wiley-VCH, **1993**.
- [50]Zeng Y F, Zhao J P, Hu B W, et al. *Chem. Eur. J.*, **2007**,**13**: 9924-9930